Adsorption 11: 65–75, 2005

Correlation of Adsorption Equilibrium Data for Water Vapor on F-200 Activated Alumina

JOSHUA D. MOORE* AND ATANAS SERBEZOV†
Department of Chemical Engineering, Rose-Hulman Institute of Technology, Terre Haute, IN 47803
serbezov@rose-hulman.edu

Received May 14, 2004; Revised January 20, 2005; Accepted February 8, 2005

Abstract. Single component adsorption equilibrium data for water vapor on commercially available activated alumina F-200 measured in a previous study (Serbezov, 2003) is correlated by two adsorption isotherm equations, both of which are based on the adsorption potential theory. The first equation is the well known Dubinin-Astakhov (D-A) equation. The second equation is obtained from a methodology proposed by Kotoh et al. (1993). It is referred to as a dual mechanism adsorption potential (DMAP) equation because it is a linear combination of two D-A terms with $n = 1$ where each term accounts for a specific mechanism of water retention. The D-A equation has two fitting parameters; the DMAP equation has three fitting parameters. The DMAP model provides a better fit for the adsorption data than the D-A model, while neither model describes the desorption data well. Analysis of the DMAP equation parameters shows that most of the water is retained by virtue of capillary condensation. In addition to fitting the experimental data, the heat of adsorption was calculated as function of the relative humidity and adsorbent loading. When capillary condensation is present, the heat of adsorption is only slightly higher than the latent heat of vaporization.

Keywords: activated alumina, water vapor, adsorption equilibrium models, adsorption potential theory, heat of adsorption

Introduction

Activated alumina desiccants are widely applied in the drying of compressed air, natural gas, and saturated hydrocarbons. In recent years one type of activated alumina with a trade name F-200 is rapidly becoming the industry standard for drying compressed air by pressure swing adsorption (PSA). In an earlier study Serbezov (2003) obtained pure component adsorption isotherm data of water vapor on F-200 activated alumina at several temperatures. The purpose of the current work is to correlate the experimental data with appropriate adsorption isotherm models and render them in a form, in which they can be applied in process modeling and simulation. An additional goal is to use the correlated data and determine the heat of adsorption.

The design of PSA units is often facilitated by the use of dynamic adsorber models (Serbezov and Sotirchos, 1997, 1999). These models require information for the adsorption equilibrium in the form of an adsorption isotherm equation that calculates the equilibrium loading at given temperature and pressure. The non-isothermal models also require information for the heat of adsorption as function of the loading.

The number of isotherm equations that are suitable for describing the adsorption of vapors on porous adsorbents over the full partial pressure range is not very large. The Dubinin-Astakhov (D-A) equation has been the most widely used equation to describe the adsorption of vapors on porous adsorbents (Do, 1998). Its

*Current address: Department of Chemical and Biomolecular Engineering, North Carolina State University, Raleigh, NC 27695.
†To whom correspondence should be addressed.

principle deficiency, however, is that at very low partial pressures it has an incorrect Henry's law behavior (Do, 1998). A correlation that has the correct Henry's law behavior at low partial pressures was proposed by Hacskaylo and LeVan (1985) using a modified Antoine equation but it has been used mostly for adsorption of light hydrocarbons on activated carbon (Al-Muhtaseb et al., 2000). Kim et al. (2003) used the Aranovich-Donohue equation and the n-layer BET equation to correlate adsorption equilibrium data of water vapor on alumina, zeolite 13X and a zeolite/activated carbon composite. Desai et al. (1992) used a combined Langmuir/BET model to correlate adsorption equilibrium data for water vapor on several types of activated alumina. Kotoh et al. (1993) developed a multilayer/multimechanism model for water adsorption on activated alumina that provided a very good fit to their experimental data.

In this work two equations are used to correlate the experimental data of water vapor on F-200 activated alumina. The first one is the D-A equation. The second one is based on the methodology described by Kotoh et al. (1993) and will be referred to as the dual mechanism adsorption potential (DMAP) equation. It is based on the adsorption potential theory and accounts explicitly for the different mechanisms by which water is held on activated alumina adsorbents. The isotherm equations are also used to calculate the heat of adsorption as function of the relative humidity and the fractional loading of the adsorbent.

Theory

Polanyi's potential theory is widely used to correlate the adsorption of vapors on porous adsorbents. It allows adsorption isotherms at different temperatures to be characterized with a single curve with respect to adsorption potential, A:

$$A = R_g T \ln\left(\frac{P_o(T)}{P}\right) \tag{1}$$

where P and $P_o(T)$ are the equilibrium and saturation pressures respectively, R_g is the ideal gas law constant, and T is the absolute temperature. The Dubinin-Astakhov (D-A) equation (Do, 1998) relates the adsorption potential to the loading in a porous adsorbent:

$$q = q_s \exp\left[-\left(\frac{A}{E}\right)^n\right]. \tag{2}$$

In Eq. (2) q is the equilibrium molar loading, q_s is the maximum molar loading, E is the characteristic energy of adsorption, and n is a heterogeneity parameter related to the pore size distribution of the adsorbent. The maximum molar loading (q_s) can be calculated from the total pore volume of the adsorbent, V_m, which can be determined by experimental methods:

$$q_s = \frac{V_m \rho}{MW}. \tag{3}$$

In Eq. (3) ρ is the liquid density of the adsorbed species, and MW is its molecular weight. The two remaining parameters in the D-A equation (E and n) can be found by fitting experimental data. When Eq. (1) is substituted in Eq. (2), a form of the D-A equation is obtained in which the equilibrium molar loading is expressed as function of the adsorbate partial pressure at constant temperature:

$$q = q_s \exp\left\{-\left(\frac{R_g T}{E}\right)^n\left[\ln\left(\frac{P_o(T)}{P}\right)\right]^n\right\}. \tag{4}$$

One deficiency of the D-A equation is that it does not distinguish between the different mechanisms by which water is retained on activated alumina. There are three distinct mechanisms that contribute to the adsorption of water vapor on activated alumina (Desai et al., 1992). At low partial pressures, water molecules chemisorb to the surface of the adsorbent. At intermediate partial pressures, water molecules physisorb to the chemisorbed water molecules. At higher partial pressures the pores are filled with liquid by capillary condensation. Kotoh et al. (1993) presented a methodology to extend the adsorption potential theory to situations with more than one adsorption mechanism. It is based on a variation of the D-A equation with $n = 1$, which effectively reduces the D-A equation to the Freundlich isotherm equation. In this study, we have used the approach of Kotoh et al. (1993) and have postulated the following adsorption isotherm equation:

$$q = q_{s1} \exp\left(-\frac{A}{E_1}\right) + (q_{s2} - q_{s1}) \exp\left(-\frac{A}{E_2}\right). \tag{5}$$

In Eq. (5) q_{s1} is the maximum molar loading due to the combined contribution of chemisorption and physisorption. The parameter q_{s2} is the maximum total molar loading due to all mechanisms and is the same as the parameter q_s in the D-A equation. The difference $(q_{s2} - q_{s1})$ is the maximum molar loading due to

capillary condensation alone. The first term in Eq. (5) accounts for the combined effect of chemisorption and physisorption, while the second term accounts for capillary condensation. Thus, we will refer to Eq. (5) as the dual mechanism adsorption potential (DMAP) equation. Following the terminology introduced by Kotoh et al. (1993), we will refer to the first term as the $j = 1$ term and the second term as the $j = 2$ term. We have combined the chemisorption and physisorption mechanisms because in our experimental data, we can only observe the combined effect of the two mechanisms. This will be explained in greater detail later in the article.

The DMAP equation has three fitting parameters: q_{s1}, E_1, and E_2. The fourth parameter q_{s2} is found from the pore volume of the adsorbent as explained earlier in Eq. (3). When Eq. (1) is substituted in Eq. (5), a form of the DMAP equation is obtained in which the equilibrium molar loading is a function of the adsorbate pressure at constant temperature:

$$q = q_{s1}\left(\frac{P}{P_o(T)}\right)^{\frac{R_g T}{E_1}} + (q_{s2} - q_{s1})\left(\frac{P}{P_o(T)}\right)^{\frac{R_g T}{E_2}}. \quad (6)$$

Eq. (6) shows that in effect the DMAP equation is a linear combination of two Freundlich type isotherms.

The heat of adsorption, $(-\Delta H)$, can be found through the van't Hoff equation:

$$\frac{(-\Delta H)}{R_g T^2} = \left(\frac{\partial \ln P}{\partial T}\right)_q. \quad (7)$$

We show in Appendix A that for both equations, D-A and DMAP, the partial derivative on the right hand side of Eq. (7) is equal to

$$\left(\frac{\partial \ln P}{\partial T}\right)_q = \left[\frac{d \ln(P_o(T))}{dT} + \frac{\ln\left(\frac{P_o(T)}{P}\right)}{T}\right]. \quad (8)$$

The first term on the right hand side of Eq. (8) can be found from the Clausius-Clapeyron equation:

$$\frac{d \ln P_o(T)}{dT} = \frac{\Delta H_{vap}(T)}{R_g T^2}, \quad (9)$$

where $\Delta H_{vap}(T)$ is the heat of vaporization at temperature T. Combining Eqs. (7)–(9) we get the following expression for the heat of adsorption:

$$-\Delta H = \Delta H_{vap}(T) + R_g T \ln\left(\frac{P_o(T)}{P}\right) = \Delta H_{vap}(T) + A. \quad (10)$$

It is seen that the heat of adsorption is a sum of the heat of vaporization and the adsorption potential. It is also seen from Eq. (10) that at constant temperature the heat of adsorption is a function of pressure only and is independent of any fitting parameters.

If more than two adsorption mechanisms are considered, additional terms can be added to the DMAP equation, which would improve the fit. The general form of the extended DMAP equation with N different terms is shown in Eq. (A6) in Appendix A. However, the heat of adsorption would always be calculated through Eq. (10) regardless of the number of terms in the extended DMAP equation.

For the D-A equation the adsorption potential A can be expressed as an explicit function of the fractional loading, θ:

$$A = E\left[\ln\frac{1}{\theta}\right]^{1/n} \quad (11)$$

where,

$$\theta = \frac{q}{q_s}. \quad (12)$$

Combining Eqs. (10) and (11), the common expression for the heat of adsorption based on the D-A equation is obtained (Do, 1998):

$$-\Delta H = \Delta H_{vap}(T) + E\left[\ln\left(\frac{1}{\theta}\right)\right]^{1/n}. \quad (13)$$

Equation (13) shows the heat of adsorption as an explicit function of the loading. For the DMAP equation, a similar expression cannot be derived because the adsorption potential is not an explicit function of the loading. For the DMAP equation, the heat of adsorption can be related to the loading numerically since the loading and the heat of adsorption are both known functions of the partial pressure (Eqs. (6) and (10)).

Experimental

The adsorption equilibrium data presented in this study was obtained by the static gravimetric technique. The adsorption equipment was IGA-002 (Intelligent Gravimetric Analyzer) system manufactured by Hiden Analytical, Ltd. (UK). The microbalance has a sample capacity of 200 mg and a weighting resolution of 0.1 μg. The temperature in the vicinity of the sample is measured by a platinum resistance thermometer

Table 1. Physical properties of F-200 7 × 14 Tyler mesh activated alumina adsorbent as reported by the manufacturer.

Form	Spherical
Diameter	2 mm
Surface area	360 m^2/g
Total pore volume	0.5 cm^3/g
Packed bulk density	769 kg/m^3

with accuracy of ±0.1°C. The pressure is measured by a capacitance manometer with a range of 100 mbar and accuracy of ±0.02 mbar. The experimental setup is described in greater detail in an earlier publication (Serbezov, 2003).

The physical properties of the F-200 activated alumina used in this study are listed in Table 1 as reported by the manufacturer's specifications for the lot. Several samples from the lot were tested for surface area and total pore volume, and the results were consistent with the manufacturer's specifications.

Results

The loading of the adsorbent as function of the adsorption potential is shown in Figs. 1 and 2 for adsorption and desorption, respectively. The experimental data is in the range from 5 to 35°C and is obtained in an earlier work (Serbezov, 2003). It is fitted to the D-A equation (Eq. (2)) using a non-linear regression routine and to the DMAP equation (Eq. (5)) using a non-linear regression routine and a linear procedure developed by Kotoh et al. (1993) described in Appendix B.

The best-fit values of the regression parameters and their standard errors are listed in Table 2 for the D-A equation and in Table 3 for the DMAP equation. The standard errors assess the precision of the best-fit values and can be used to compute confidence intervals (Motulsky and Christopoulos, 2003). For all parameters listed in Tables 2 and 3, the 95% confidence interval (i.e., the interval that has a 95% probability of containing the true value of the parameter) is centered at the best-fit value and extends two standard errors on both sides (above and below).

The 95% confidence intervals for the DMAP parameters obtained by the linear and non-linear regression procedures overlap significantly, which is an indication that the two procedures can be statistically considered equivalent. Since the non-linear regression is much easier to set up, it is recommended for future studies.

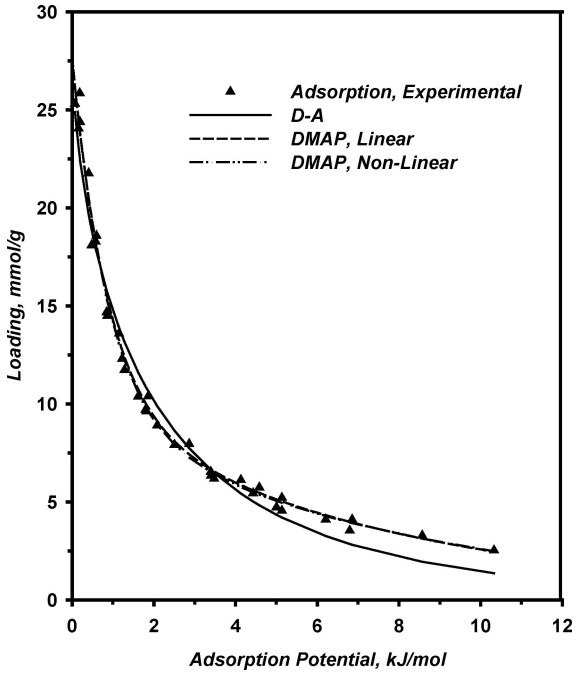

Figure 1. D-A and DMAP equation adsorption potential fits for adsorption data in the range from 5 to 35°C.

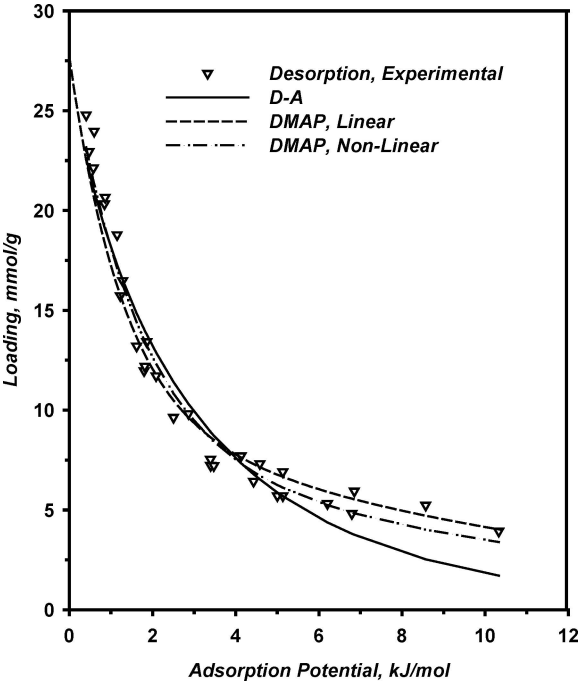

Figure 2. D-A and DMAP equation adsorption potential fits for desorption data in the range from 5 to 35°C.

Table 2. D-A equation parameters for adsorption and desorption in the range from 5 to 35°C.

	Adsorption	Desorption
q_s (Std. Error), mmol/g	27.709 (1.574)	27.709 (3.213)
E (Std. Error), kJ/mole	1.993 (0.218)	2.905 (0.504)
n (Std. Error)	0.670 (0.064)	0.807 (0.144)

Table 3. DMAP equation parameters for adsorption and desorption in the range from 5 to 35°C.

	$q_{s,j}$ (Std. Error) mmol/g		E_j (Std. Error) kJ/mol	
j	Linear procedure	Non-Linear procedure	Linear procedure	Non-Linear procedure
	Adsorption			
1	10.018 (1.318)	9.643 (1.255)	7.355 (1.369)	7.606 (1.44)
2	27.709 (0.499)	27.709 (0.488)	0.862 (0.098)	0.862 (0.093)
	Desorption			
1	9.920 (4.011)	8.215 (5.244)	11.416 (7.720)	11.517 (10.731)
2	27.709 (1.952)	27.709 (1.381)	1.284 (0.442)	1.640 (0.521)

Table 4 presents a summary of the statistical measures that are used to determine which one of the two models fits the data better. The coefficient of determination (R^2) describes how close the fitted curve comes to the data. Both models have very high R^2 values indicating that they both describe the data well with the DMAP being slightly better. The standard error of estimate (SEE) quantifies the uncertainty in the regression curve and it is smaller for the DMAP model. The sum of squares (SS) is a measure of how well the model predicts the experimental data while the predicted residual error sum of squares (PRESS) is a measure of how well the model predicts new data. The lower SS and PRESS values for the DMAP model indicate that it has better predictive capabilities than the D-A model. The reason is that the D-A model does not differentiate between the different mechanisms by which water is retained on the adsorbent.

Table 4. Statistics for D-A and DMAP equation fits for adsorption and desorption in the range from 5 to 35°C.

Model	R^2	SEE	SS	PRESS	D-W
			Adsorption		
D-A	0.974	1.172	42.549	53.872	0.649
DMAP linear procedure	0.992	0.663	13.197	18.219	1.995
DMAP non-linear procedure	0.992	0.650	12.655	17.529	2.088
			Desorption		
D-A	0.947	1.571	66.630	87.270	0.523
DMAP linear procedure	0.962	1.360	48.098	67.515	0.693
DMAP non-linear procedure	0.973	1.137	33.588	46.782	0.985

The Durbin-Watson (D-W) statistic is a measure of the correlation between the residuals (i.e., the difference between the observed and predicted values). The more this value differs from 2, the greater the likelihood that the residuals are correlated, and the fit is not likely to describe the data well. In Table 4 the D-W statistic is 2 only for the DMAP fit of the adsorption data and significantly less than 2 in all other cases. This suggests that the DMAP model provides a better fit for the adsorption data than the D-A model, while neither model describes the desorption data well. The poor fit for the desorption data is also evidenced by the fact that each desorption parameter has a much larger standard error (broader confidence interval) than its corresponding adsorption parameter.

The regressed D-A and DMAP parameters can be substituted in Eqs. (4) and (6), respectively, to obtain adsorption and desorption isotherms at different temperatures. Figure 3 shows the adsorption and desorption isotherms at 25°C and compares them to the experimental data. The desorption data is poorly correlated, which is consistent with previously discussed results. It can also be seen that the DMAP equation provides a better fit to the adsorption data than the D-A equation.

The experimental data shows that a pronounced hysteresis exists in the entire range of partial pressures. This is the reason why the adsorption and desorption data are fitted separately. The hysteresis in the upper range of partial pressures (i.e., after the onset of capillary condensation) is of the H3 type, based on the IUPAC classification (Sing et al., 1985). Its characteristic feature is that the isotherm does not level off at relative pressures close to the saturation vapor pressure. This phenomenon has been observed in many experimental studies but its origin is still not fully understood. The existence of H3 type hysteresis has generally been attributed to the presence of slit-shaped pores (Rouquerol et al., 1999), but more recently it has been suggested that H3 hysteresis loops may arise from the presence of large mesopores embedded in a matrix with pores of

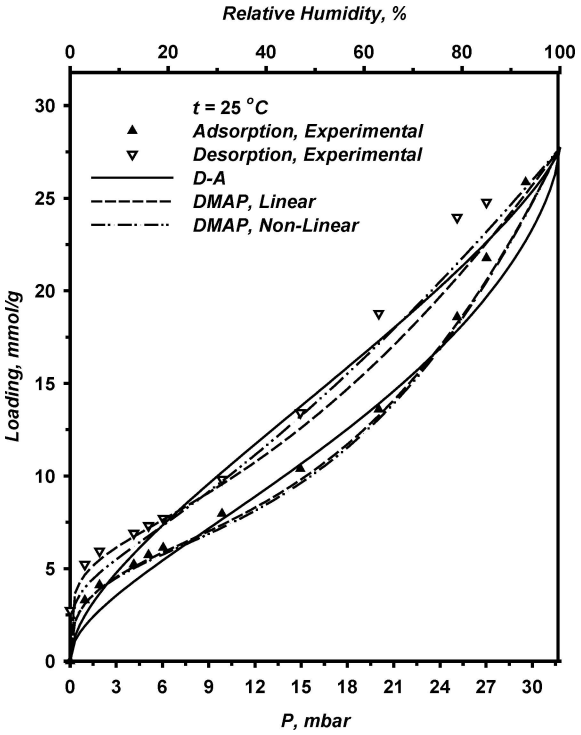

Figure 3. D-A and DMAP equation fits for adsorption and desorption at 25°C.

much smaller size (Kruk and Jaroniec, 2001). The hysteresis in the lower range of partial pressures (i.e., before the onset of capillary condensation) is most likely caused by chemisorption effects (Sing et al., 1985).

As mentioned earlier, the contributions of chemisorption and physisorption have been lumped into one mechanism represented by the first term of Eq. (5). The reason for this is that chemisorption occurs at very low partial pressures where experimental data has not been obtained, and therefore, the individual contribution of chemisorption cannot be isolated from that of physisorption. Assuming that chemisorbed water cannot be desorbed by virtue of vacuum alone, the loading at the last desorption point in the experimental sequence (10^{-6} mbar) can be viewed as representative of the maximum loading of chemisorbed water. From the experimental data in Fig. 3 for 25°C, it is seen that the loading at the first adsorption point in the experimental sequence (1 mbar) is higher than the loading at the last desorption point in the experimental sequence (10^{-6} mbar). The experimental data at all other temperatures shows the same pattern. Thus, the available experimental data reveals only the combined effect of chemisorption and physisorption, and this is why the two mechanisms have been lumped together in the DMAP equation.

The maximum molar loading due to the combined effect of chemisorption and physisorption can be estimated by examining the values of the q_{s1} parameter in the DMAP equation in Table 3. It is expected that q_{s1} be approximately the same for both adsorption and desorption. This expectation is supported by the fact that the 95% confidence interval for adsorption is completely enclosed in the 95% confidence interval for desorption. Based on the results from the non-linear procedure, it can be said with 95% confidence that the true value of q_{s1} is between 7.133 mmol/g and 12.153 mmol/g. Comparing q_{s1} to $(q_{s2} - q_{s1})$ it can be concluded that capillary condensation is the dominant mechanism by which water is held on the F-200 activated alumina.

The individual contributions of the two mechanisms in the DMAP equation are shown in Fig. 4 for adsorption at 35°C using the best-fit parameters from the non-linear procedure. It is seen that for relative humidity below 25% capillary condensation is very small and

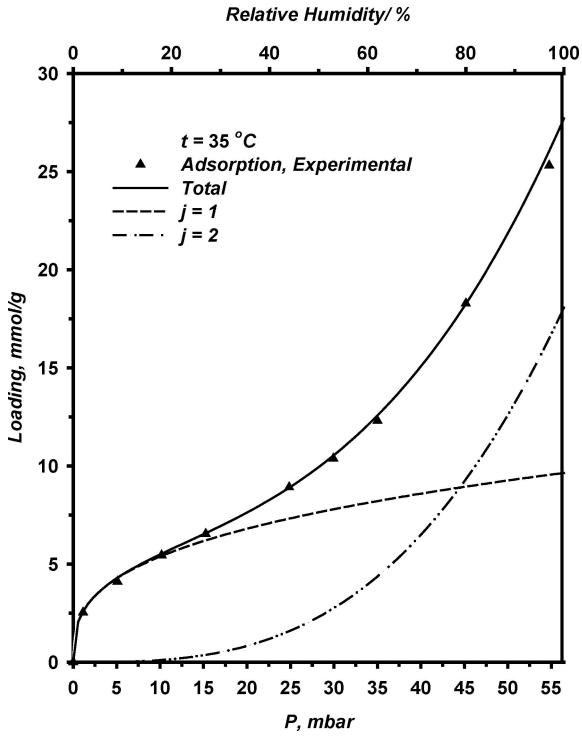

Figure 4. Contribution of the individual terms in the DMAP equation for adsorption data at 35°C.

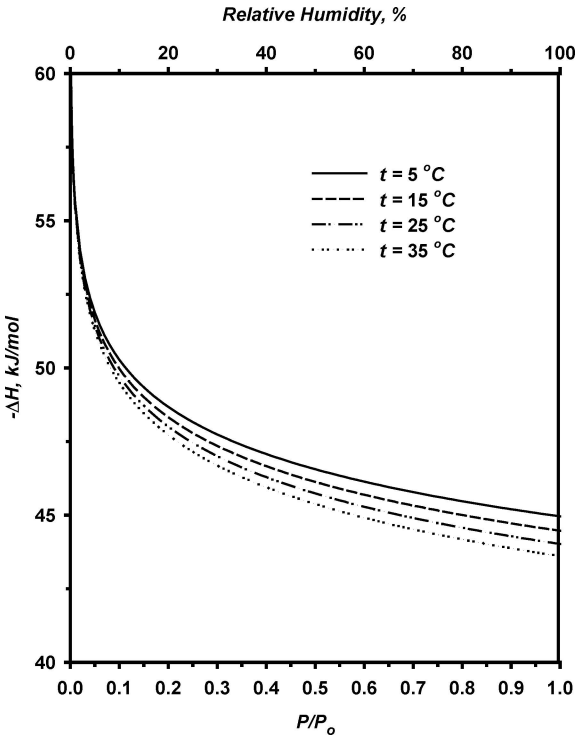

Figure 5. Heat of adsorption for the D-A and DMAP equations as a function of pressure at 5, 15, 25, and 35°C.

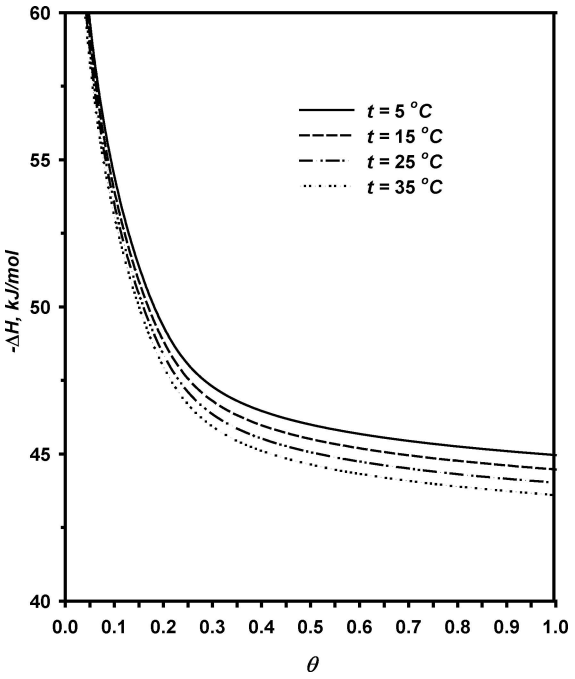

Figure 6. Heat of adsorption for the DMAP equation as a function of fractional loading at 5, 15, 25, and 35°C.

the second term in the DMAP equation can be neglected as described in Appendix B. At higher relative humidity the loading due to capillary condensation increases much faster than the loading due to chemisorption and physisorption together.

The heat of adsorption as a function of the relative humidity at different temperatures is shown in Fig. 5. The results are obtained with Eq. (10) and pertain to all desiccants whose adsorption isotherms can be represented by the D-A, the DMAP, or the extended DMAP equations. Since the extended DMAP equation (Eq. (A6)) can have an infinite number of fitting parameters and produce adequate fits for a broad range of desiccants, Eq. (10) and Fig. 5 are generic and can be used for a large number of adsorbents.

Figure 6 presents the heat of adsorption at different temperatures as a function of fractional loading predicted by the DMAP equation. The results are produced by combining Eqs. (6) and (10) and using the non-linear regression parameters in Table 3.

It follows from Eq. (10) that at saturation the heat of adsorption is equal to the heat of vaporization. Figure 5 shows that in the range of pressures where capillary condensation occurs (relative humidity above 25%) the heat of adsorption is not very much higher (less than 7%) than the heat of vaporization. Figure 6 presents the same results in terms of fractional loading. When $\theta = 0.25$ the heat of adsorption is only 7% higher than the heat of vaporization, and this difference decreases as the loading increases. At very low pressures, the heat of adsorption becomes unbound, which results from the fact that both the D-A and the DMAP equations do not have the correct Henry's law behavior at very low pressures.

Conclusions

The adsorption equilibrium of water vapor on commercially available activated alumina F-200 was correlated by the D-A and the DMAP equations. The latter is a linear combination of two Freundlich isotherms: one accounting for the water retention due to the combined effects of chemisorption and physisorption and the other accounting for the water held on the adsorbent by capillary condensation. Chemisorption and physisorption were lumped in a single term because their

individual contributions could not be distinguished in the experimental data. Of the two equations, the DMAP equation provided a much better fit to the adsorption data, while neither model described the desorption data well.

The parameters in the DMAP equation were fitted using linear and non-linear regression techniques. Both methods were determined to be statistically equivalent, and the non-linear technique was recommended for future studies because it was easier to apply. Based on the physical meaning of the DMAP equation parameters it was concluded that capillary condensation was the dominant mechanism by which water was held on the adsorbent.

Capillary condensation was determined to be significant above approximately 25% relative humidity and 25% fractional loading. The heat of adsorption as function of the relative humidity and the fractional loading was also calculated. For relative humidity or fractional loadings where capillary condensation was present, the heat of adsorption was only slightly higher (7% or less) than the heat of vaporization.

The results presented in this study were based on the assumption of constant water density—the average density in the temperature range of interest, 5 to 35°C. The calculations were repeated by taking into account the water density change with temperature, but there was no significant difference in the results. This was consistent with the fact that water density is a weak function of temperature and the temperature range of interest was very narrow, only 30°C.

The F-200 activated alumina is a very popular adsorbent in industrial practice. Many PSA plants, either in operation or under design considerations, use this adsorbent for water vapor removal from various gas streams. The design and the optimization of these units involve the use of dynamic simulation models of different degrees of complexity. A common requirement for the application of these models, even the simplest ones, is the availability of adsorption equilibrium data regressed to an appropriate adsorption isotherm equation. Thus, the correlations presented in this study can be applied in design and the optimization of adsorption columns packed with F-200 activated alumina and used for water vapor removal.

Nomenclature

A	Adsorption potential defined in Eq. (1), kJ/mol
E	Characteristic energy in the D-A equation (Eq. (2)), kJ/mol
E_1	Characteristic energy in the DMAP equation (Eq. (5)) for the $j = 1$ term, kJ/mol
E_2	Characteristic energy in the DMAP equation (Eq. (5)) for the $j = 2$ term, kJ/mol
$(-\Delta H)$	Heat of adsorption, kJ/mol
$\Delta H_{vap}(T)$	Heat of vaporization of water at temperature T, kJ/mol
j	Number that designates the retention mechanism in the DMAP equation (Eq. (5)); chemisorption and physisorption ($j = 1$) or capillary condensation ($j = 2$)
MW	Molecular weight of the adsorbed species
n	Heterogeneity parameter in the D-A equation (Eq. (2)) related to pore size distribution
N	Counter in extended DMAP equation (Eq. (A6))
P	Partial pressure of water, mbar
$P_o(T)$	Saturation pressure of water at temperature T, mbar
q	Equilibrium molar loading, mmol/g
q_s	Maximum molar loading in the D-A equation (Eq. (2)), mmol/g
q_{s1}	Maximum molar loading for the $j = 1$ term in the DMAP equation (Eq. (5)), mmol/g
q_{s2}	Maximum total loading in the DMAP equation (Eq. (5)), mmol/g
R_g	Ideal gas law constant, kJ/mol-K
t	Temperature, °C
T	Absolute temperature, °K
V_m	Pore volume of adsorbent, cm^3/g

Greek letters

θ	fractional loading defined in Eq. (12)
ρ	liquid density of the adsorbed species, cm^3/g

Other

D-A	Dubinin-Astakhov
DMAP	Dual Mechanism Adsorption Potential
D-W	Durbin Watson statistic
PRESS	Predicted residual error sum of squares
PSA	Pressure swing adsorption
R^2	Coefficient of determination
SEE	Standard error of estimate
SS	Sum of squares

Appendix A: Calculation of the $(\frac{\partial \ln P}{\partial T})_q$ Term in the van't Hoff Equation for the D-A, the DMAP and the Extended DMAP Equations

Since the molar loading q is a function of temperature and pressure, (i.e., $q\,(T,\,P)$) we apply the rules of multivariable calculus to get

$$\left(\frac{\partial \ln P}{\partial T}\right)_q = \frac{1}{P}\left(\frac{\partial P}{\partial T}\right)_q = -\frac{\left(\frac{\partial q}{\partial T}\right)_P}{P\left(\frac{\partial q}{\partial P}\right)_T}. \quad \text{(A1)}$$

For the D-A equation (Eq. (4)) the corresponding partial derivatives are

$$\left(\frac{\partial q}{\partial T}\right)_p = -nq_s \exp\left\{-\left(\frac{R_gT}{E}\right)^n\left[\ln\frac{P_o(T)}{P}\right]^n\right\} \times\left(\frac{R_gT}{E}\right)^n\left[\ln\frac{P_o(T)}{P}\right]^n\left(\frac{1}{T}+\frac{\frac{d\ln P_o(T)}{dT}}{\ln\left(\frac{P_o(T)}{P}\right)}\right). \quad \text{(A2)}$$

and

$$\left(\frac{\partial q}{\partial P}\right)_T = \frac{nq_s \exp\left\{-\left(\frac{(R_gT)}{E}\right)^n\left[\ln\frac{P_o(T)}{P}\right]^n\right\}\left(\frac{R_gT}{E}\right)^n\left[\ln\frac{P_o(T)}{P}\right]^n}{P\ln\left(\frac{P_o(T)}{P}\right)}. \quad \text{(A3)}$$

When Eqs. (A2) and (A3) are substituted into Eq. (A1) and the resulting expression is simplified, the result shown in Eq. (8) is obtained.

For the DMAP equation (Eq. (6)) the corresponding partial derivatives are

$$\left(\frac{\partial q}{\partial T}\right)_P = -\left[R_gT\left(\frac{d\ln P_o(T)}{dT}\right)+R_g\ln\left(\frac{P_o(T)}{P}\right)\right] \times\left(q_{s_1}\frac{\left(\frac{P}{P_o(T)}\right)^{\frac{R_gT}{E_1}}}{E_1}+\left(q_{s_2}-q_{s_1}\right)\frac{\left(\frac{P}{P_o(T)}\right)^{\frac{R_gT}{E_2}}}{E_2}\right). \quad \text{(A4)}$$

and

$$\left(\frac{\partial q}{\partial P}\right)_T = \frac{R_gT}{P}\left(q_{s_1}\frac{\left(\frac{P}{P_o(T)}\right)^{\frac{R_gT}{E_1}}}{E_1}+\left(q_{s_2}-q_{s_1}\right) \times\frac{\left(\frac{P}{P_o(T)}\right)^{\frac{R_gT}{E_2}}}{E_2}\right). \quad \text{(A5)}$$

When Eqs. (A4) and (A5) are substituted into Eq. (A1) and the resulting expression is simplified, the result shown in Eq. (8) is obtained.

If more than two adsorption mechanisms are considered, the DMAP equation can be extended to include additional terms. The general form of the extended DMAP equation with N different terms is

$$q = q_{s_1}\left(\frac{P}{P_o(T)}\right)^{\frac{R_gT}{E_1}} + \sum_{j=2}^{N}\left[\left(q_{s_j}-q_{s_{j-1}}\right)\left(\frac{P}{P_o(T)}\right)^{\frac{R_gT}{E_j}}\right]. \quad \text{(A6)}$$

The partial derivatives with respect to temperature and pressure are

$$\left(\frac{\partial q}{\partial T}\right)_P = -\left[R_gT\left(\frac{d\ln P_o(T)}{dT}\right)+R_g\ln\left(\frac{P_o(T)}{P}\right)\right] \times\left[q_{s_1}\frac{\left(\frac{P}{P_o(T)}\right)^{\frac{R_gT}{E_1}}}{E_1}+\sum_{j=2}^{N}\left(q_{s_j}-q_{s_{j-1}}\right) \times\frac{\left(\frac{P}{P_o(T)}\right)^{\frac{R_gT}{E_j}}}{E_j}\right]. \quad \text{(A7)}$$

and

$$\left(\frac{\partial q}{\partial P}\right)_T = \frac{R_gT}{P}\left(q_{s_1}\frac{\left(\frac{P}{P_o(T)}\right)^{\frac{R_gT}{E_1}}}{E_1} + \sum_{j=2}^{N}\left(q_{s_j}-q_{s_{j-1}}\right)\frac{\left(\frac{P}{P_o(T)}\right)^{\frac{R_gT}{E_j}}}{E_j}\right). \quad \text{(A8)}$$

When Eqs. (A7) and (A8) are substituted into Eq. (A1) and the resulting expression is simplified, the result shown in Eq. (8) is obtained.

Appendix B: Linear Regression Procedure for the DMAP Equation

At low pressure, the contribution of capillary condensation ($j = 2$ term) is small and can be assumed negligible. With this assumption, Eq. (5) simplifies to:

$$q = q_{s1}\exp\left(-\frac{A}{E_1}\right). \quad \text{(B1)}$$

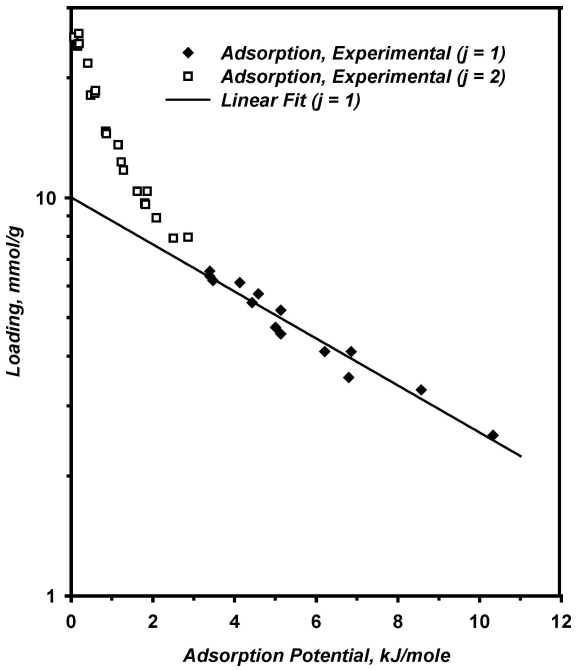

Figure B1. DMAP equation adsorption potential fit for the $j = 1$ term in Eq. (5) for the adsorption data in the range from 5 to 35°C.

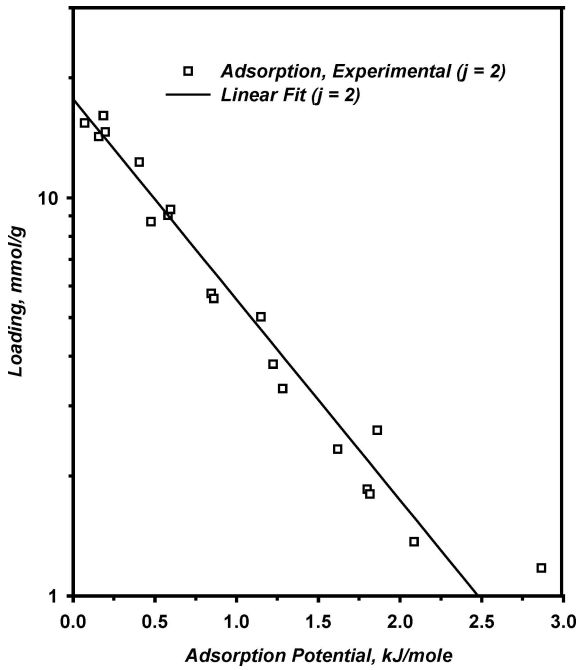

Figure B2. DMAP equation adsorption potential fit for the $j = 2$ term in Eq. (5) for the adsorption data in the range from 5 to 35°C.

On a semi-logarithmic scale, the loading due to the combined effect of chemisorption and physisorption ($j = 1$ term) shows a linear relationship with respect to adsorption potential. The values of q_{s1} and E_1 can be determined from the intercept and the slope of the line, respectively. This is shown in Fig. B1 for the adsorption data. The desorption data was fit in the same manner. Next, the contribution of capillary condensation at higher partial pressures is found by rearranging Eq. (5):

$$q - q_{s1} \exp\left(-\frac{A}{E_1}\right) = (q_{s2} - q_{s1}) \exp\left(-\frac{A}{E_2}\right). \tag{B2}$$

When the left hand side of Eq. (B2) is plotted versus the adsorption potential on a semi-logarithmic scale, an equation of a straight line is obtained, and E_2 can be determined from the slope of the line. The intercept of the line is fixed since the values of q_{s2} and q_{s1} are already known. The DMAP equation correlation for the $j = 2$ term is shown in Fig. B2 for the adsorption data, and the desorption data was fit in the same manner.

References

Al-Muhtaseb, S.A., M.D. LeVan, and J.A. Ritter, "On the Correlation of Modified Antoine's Adsorption Isotherm Models with Experimental Data," *Langmuir*, **16**, 8536–8538 (2000).

Desai, R., M. Hussain, and D.M. Ruthven, "Adsorption of Water Vapor on Activated Alumina," *Can. J. Chem. Eng.*, **70**, 699–706 (1992).

Do, D.D., *Adsorption Analysis: Equilibrium and Kinetics*, Chapter 4, Imperial College Press, London, 1998.

Hacskaylo, J.J. and M.D. LeVan, "Correlation of Adsorption Equilibrium Data Using a Modified Antoine Equation: A New Approach for Pore-Filling Models," *Langmuir*, **1**, 97–100 (1985).

Kim, J.H., C.H. Lee, W.S. Kim, J.S. Lee, J.T. Kim, J.K. Suh, and J.M. Lee, "Adsorption Equilibria of Water Vapor on Alumina, Zeolite 13X, and a Zeolite X/Activated Carbon Composite," *J. Chem. Eng. Data*, **48**, 137–141 (2003).

Kotoh, K., M. Enoeda, T. Matsui, and M. Nishikawa, "A Multilayer Model for Adsorption of Water on Activated Alumina in Relation to Adsorption Potential," *J. Chem. Eng. Japan*, **26**, 355–360 (1993).

Kruk, M. and M. Jaroniec, "Gas Adsorption Characterization of Ordered Organic-Inorganic Nanocomposite Materials," *Chem. Mater.* **13**, 3169–3183 (2001).

Motulsky, H.J. and A. Christopoulos, *Fitting Models to Biological Data Using Linear and Nonlinear Regression: A Practical Guide to Curve Fitting*, GraphPad Software, Inc., San Diego, CA, 2003.

Rouquerol, F., J. Rouquerol, and K. Sing, *Adsorption by Powders and Porous Solids*, Academic Press, San Diego, CA, 1999.

Sing, K.S.W., D.H. Everett, R.A.W. Haul, L. Moscou, R.A. Pierotti, J. Rouquerol, and T. Siemieniewska, "Reporting Physisorption Data for Gas/Solid Systems with Special Reference to the Determination of Surface Area and Porosity," *Pure Appl. Chem*., **57**, 603–619 (1985).

Serbezov, A., "Adsorption Equilibrium of Water Vapor on F-200 Activated Alumina," *J. Chem. Eng. Data*. **48**, 421–425 (2003).

Serbezov, A. and S.V. Sotirchos, "Mathematical Modeling of the Adsorptive Separation of Multicomponent Gaseous Mixtures," *Chem. Eng. Sci*., **52**, 79–91 (1997).

Serbezov, A. and S.V. Sotirchos, "Particle-Bed Model for Multicomponent Adsorption-Based Separations: Application to Pressure Swing Adsorption," *Chem. Eng. Sci*., **54**, 5647–5666 (1999).